Gem News International

Contributing Editors
Emmanuel Fritsch, *University of Nantes, CNRS, Team 6502, Institut des Matériaux Jean Rouxel (IMN), Nantes, France* (fritsch@cnrs-imn.fr)
Gagan Choudhary, *Gem Testing Laboratory, Jaipur, India* (gagan@gjepcindia.com)
Christopher M. Breeding, *GIA, Carlsbad* (christopher.breeding@gia.edu)

COLORED STONES AND ORGANIC MATERIALS

A near-field-communication (NFC) technology device embedded in bead cultured pearls. The Carlsbad laboratory received for examination two dark-colored bead cultured pearls embedded with an electronic device (figure 1) from Jeremy Shepherd, CEO of Pearl Paradise. The first sample had been cut in half by Mr. Shepherd in order to investigate the interior components; the smaller half weighed 2.56 ct and measured 10.63 × 9.73 × 3.88 mm (figure 1, left), and the larger half weighed 4.46 ct and measured 10.84 × 10.20 × 5.48 mm (figure 1, center). The second sample (figure 1, right) was intact and weighed 7.83 ct, measuring 10.84 × 10.20 × 5.48 mm. Both samples exhibited the typical external appearance of bead cultured pearls produced by the *Pinctada margaritifera* mollusk (referred to in the trade as "Tahitian" or "Black South Sea"). UV-Vis spectra of these samples showed the characteristic reflectance features typical of naturally colored pearls originating from this mollusk, with identifying features recorded at 405, 495, and 700 nm.

The cross-section surfaces of the two halves showed a straightforward bead cultured pearl structure. A round translucent white shell bead nucleus was clearly visible in the center. Its freshwater origin was subsequently verified with optical X-ray fluorescence imaging and EDXRF analysis. The alternating cream and brown concentric layers immediately overgrowing the bead were a combination of calcium carbonate and organic-rich materials (i.e., conchiolin) that are sometimes produced during the initial growth stage prior to nacre (aragonite) deposition. The subsequently deposited layers are dark-colored nacre commonly produced by the *P. margaritifera* mollusk. An electronic device was very obvious within a large partial drill hole that ran through the bead and into the other side of nacre.

Real-time microradiography (RTX) revealed that the electronic devices embedded in the two halves and in the intact pearl samples were of the same kind. The device was composed of a high-density radio-opaque core (measuring approximately 5.10 × 3.26 mm) that appeared white in the RTX image and as an opaque black filler in the cross sections. An antenna could be seen wrapped around the core, and a circuit board was connected to the end of the antenna (figure 2). Chemical analysis of these components using laser ablation–inductively coupled plasma–mass spectrom-

Figure 1. An intact 7.83 ct Pinctada margaritifera *bead cultured pearl (right), together with a sectioned sample (2.56 ct left and 4.46 ct center), embedded with a near-field-communication (NFC) chip. Photo by Diego Sanchez.*

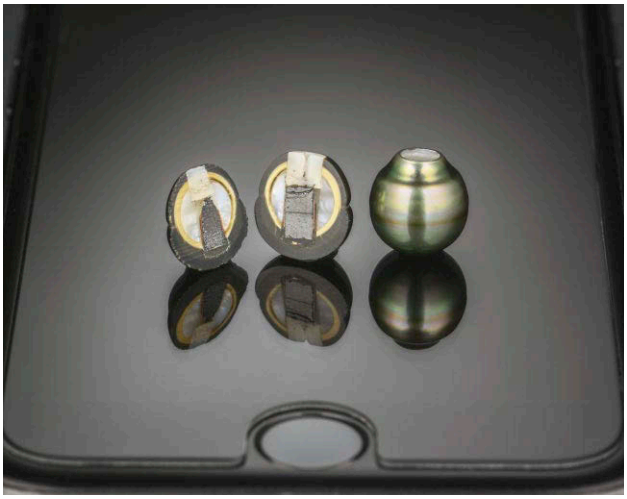

Editors' note: Interested contributors should send information and illustrations to Stuart Overlin at soverlin@gia.edu or GIA, The Robert Mouawad Campus, 5345 Armada Drive, Carlsbad, CA 92008.

Gems & Gemology, Vol. 56, No. 3 pp. 436–445.

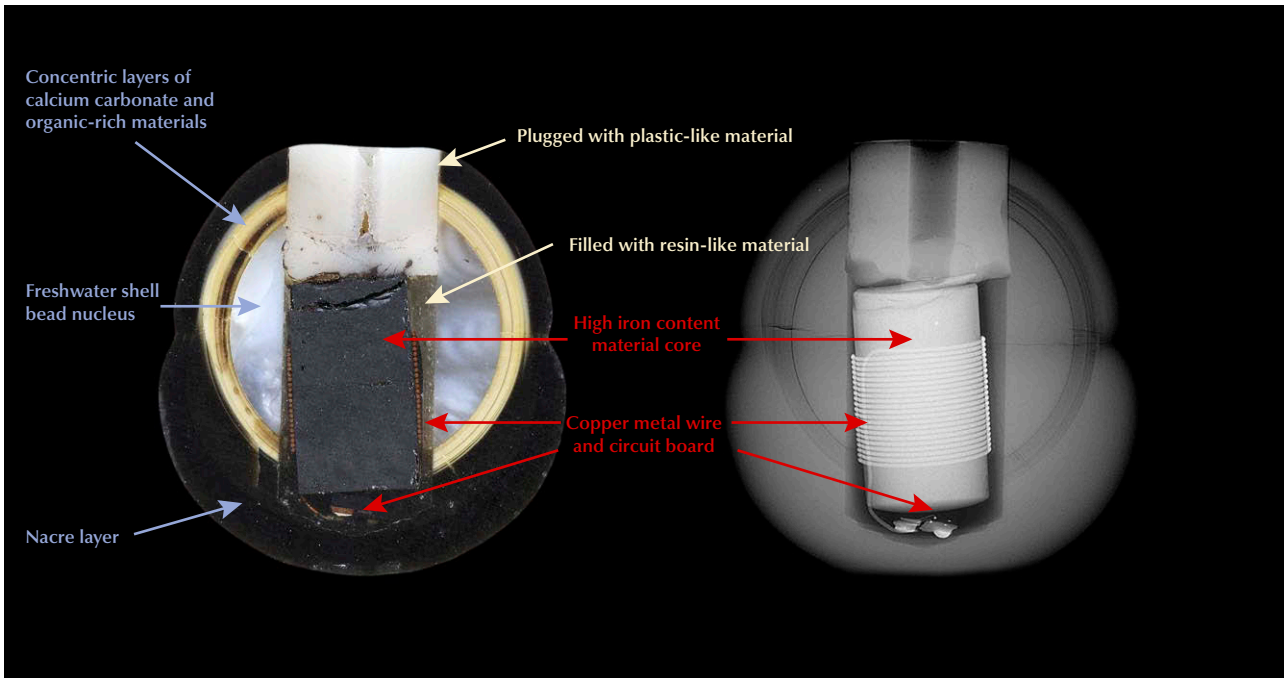

Figure 2. The cross section (left) and microradiograph (right) images of the same sample revealed the varied components of the bead cultured pearl and NFC chip. Photos by Diego Sanchez (left) and Artitaya Homkrajae (right).

etry (LA-ICP-MS) revealed that the black core was composed of a high-iron (Fe) material, which was confirmed using a magnet. The bronze-colored antenna and circuit board were identified as copper. The device was held in place in the large drill hole with a transparent near-colorless resin-like material containing numerous gas bubbles. The drill hole areas were worked (cut) to a flattened surface and plugged with a white plastic-like material, which was subsequently re-drilled with a smaller drill hole. Although the large drill hole was placed in the center, it did not affect the origin determination of the pearl. The shell bead nucleus and the device contained within could be observed using RTX, even for the intact sample. The pearl's shape was certainly impacted by the cut surface, and the classifications for color, overtone, luster, and surface would be based on the remaining nacreous surface.

The electronic device appeared to be a near-field-communication (NFC) chip, which is a short-range wireless connectivity technology based on traditional radio-frequency identification (RFID) (https://nfc-forum.org/what-is-nfc/about-the-technology). NFC technology allows data transfer between two NFC-enabled devices through electromagnetic radio fields within a very short distance, either by physically touching or being within a few centimeters of each other. NFC chips are passive and do not need to have a power source of their own, though the antenna can be coupled with an active device such as a smartphone via an electromagnetic field. The chip is used to store digital information such as images, video, text, and audio, which are accessed through an app due to limited memory. To the best of our knowledge, this technology was first incorporated within pearl jewelry by Galatea: Jewelry by Artist and marketed under the name "Momento" (https://www.momentogem.com). However, the NFC chip embedded in the intact pearl sample in this study was not compatible with the Galatea Momento smartphone application.

So far, GIA has observed three kinds of electronic devices in cultured pearls. The first device encountered was an RFID chip implanted inside a shell nucleus by Fukai Shell Nucleus prior to the culturing process ("ID nuclei add value to pearls," *Hong Kong Jewellery*, September 2013, pp. 62–64). The RFID technology is used to track and identify the pearl directly from farm to consumer. The second was a "capsule-like" feature found within an atypical *P. margaritifera* bead cultured pearl set in a ring that was submitted for identification at GIA Hong Kong, yet the reason for the device remains unknown (Spring 2020 Lab Notes, pp. 134–136). This NFC chip is the third kind and is used for wireless data transmission with an NFC-enabled device such as a mobile phone. The NFC chips were inserted into bead cultured pearls after they had been cultured, unlike the RFID chip. Therefore, the pearl is still classified as a bead cultured pearl on GIA's pearl identification report. The presence of the device is mentioned in the comments section.

Technology is pervasive in our daily lives and can even influence how pearl jewelry is produced. Since cultured pearls are opaque, the implementation of such micro-technologies within them is a viable option. These innovative wearable technologies retain the external appearance of pearls while performing a specific function.

Artitaya Homkrajae
GIA, Carlsbad

Trapiche-type emeralds from Pakistan. Numerous gem materials have been designated "trapiche" in the trade and in various publications. They generally describe a pattern consisting of a fixed non-transparent star in a transparent matrix, with the arms of the six-rayed star radiating from a central point or from a central core to the rim of the crystal. Only a limited number of mineral species show a clear trapiche pattern within crystal slices (i.e., a pattern with a clear separation of the crystal into distinct growth sectors). The boundaries of these growth sectors, running from the center to the edges between external prism or pyramidal faces, are normally sharp and contain mineral or fluid inclusions, separating different parts within the rim. These sector boundaries are also described as the arms of the fixed six-rayed star. The most prominent gem minerals showing a distinct trapiche pattern are Colombian emeralds and rubies from Myanmar.

Another group of gem materials is characterized by several areas of increased transparency and translucency that surround a central point or central core according to the symmetry of the host. The two types of areas are characterized by different concentrations of inclusions, which are trapped within specific parts of symmetry-equivalent growth sectors of the host. The arms of the fixed star are perpendicular to the external crystal faces. The most prominent gem materials of this second group are blue basaltic sapphires from different sources, but similar patterns also have been described for other gem varieties such as aquamarine from Namibia. This second group of crystals is designated "trapiche-type," and the emeralds from Pakistan described in this entry belong to this group of gem materials.

Trapiche-type emeralds originating from the Swat mining region in Pakistan have recently been described by Y. Gao et al. (Fall 2019 Gem News International, pp. 441–442) and H. Guo et al. ("Inclusion and trace element characteristics of emeralds from Swat Valley, Pakistan," pp. 336–355 of this issue). The samples showed an interesting growth pattern and color zoning with a colorless core, a lighter green intermediate zone, and a more intense green rim. The inclusions forming the trapiche-type pattern were restricted to the lighter green intermediate growth zone.

Recently, the author received six slices of similar material, reportedly from Swat, from the gem collector S. Hanken of Waldkraiburg, Germany; the samples had been purchased in 2020 from the U.S. gem trade. One of these samples, which were all cut perpendicular to the c-axis of the emerald crystals, showed an interesting growth pattern. The emerald slice measured from 4.6 to 4.8 mm (distances between different prism faces) with a thickness of 1.9 mm (figure 3). The sample revealed two colorless beryl cores of almost equal size. One of these colorless cores was surrounded by a large light green intermediate zone, which also contained the inclusions forming the trapiche-type pattern. The second core was surrounded by a lighter green intermediate zone, which was much smaller. Encompassing these two intermediate zones were intense green hexagonal growth boundaries with growth planes parallel to the external prism faces.

This intense green growth boundary surrounds both light green intermediate growth zones. Subsequent to this intense green boundary, an intense green outer rim without trapiche-type inclusions but with additional growth planes parallel to the prism faces was present.

As already described by Gao et al., the emerald was grown in three distinct steps with a colorless beryl core, a light green intermediate zone, and an intense green rim. All growth steps were separated by sharp boundaries, with a thin growth layer between the intermediate zone and the rim, which showed the most intense green coloration observed in the sample. The emerald formed with two cores, with a subsequent growth step, in which both parts were still separated from each other. Only in the last growth step, in which the intense green rim was formed, were the two parts of the final emerald crystal in contact with each other.

Karl Schmetzer
Petershausen, Germany

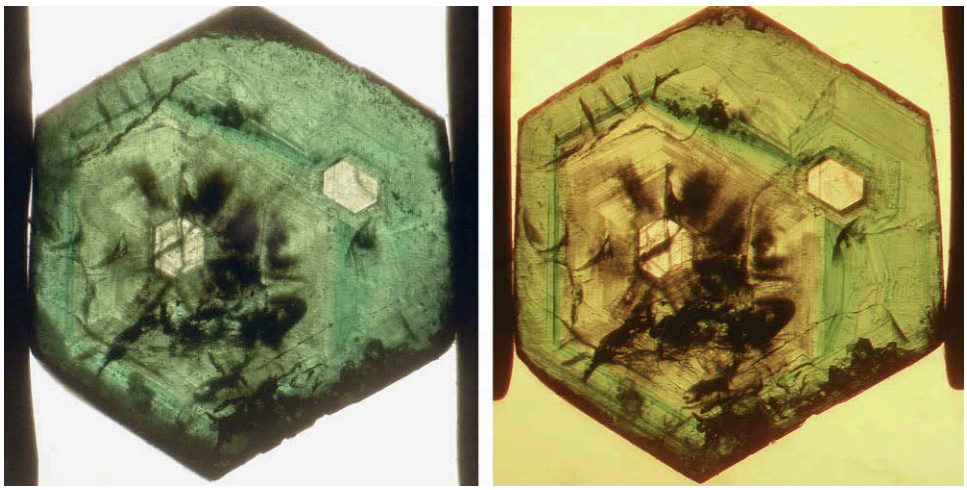

Figure 3. Growth pattern observed in a trapiche-type emerald from Swat, Pakistan. The slice shows two colorless cores and two intermediate lighter green zones surrounded by a more intense green rim. Viewed perpendicular to the c-axis, in air (left) and immersion (right); diameter of the sample from 4.6 to 4.8 mm. Photos by Karl Schmetzer.

Unusual violet Maxixe beryl. Recently examined in the Carlsbad laboratory was a 26.72 ct transparent violet modified cushion mixed-cut stone (figure 4). Standard gemological testing revealed a refractive index of 1.583–1.592 and a specific gravity of 2.78, both consistent with beryl. Using plane-polarized light, pale purple and saturated blue pleochroic colors were observed. A uniaxial optic figure was seen at the girdle, and the optical orientation of the stone showed the stronger blue pleochroic color down the optic axis direction. The stone was inert to long-wave UV light and fluoresced weak greenish yellow to short-wave UV. Viewed with fiber-optic light during microscopic examination, it displayed a few scattered blocky crystals, platelets, and needles, confirming natural growth origin. No coatings were seen on the surface under reflective light. Other than the unusual violet color, these properties were consistent with Maxixe beryl.

Advanced testing by LA-ICP-MS revealed that the stone lacked iron. This result was consistent with Maxixe beryl, in which iron is too low to be measured (I. Adamo et al., "Aquamarine, Maxixe-type beryl, and hydrothermal synthetic blue beryl: Analysis and identification," Fall 2008 *G&G*, pp. 214–226). Maxixe beryl normally has a blue to violet blue bodycolor, but this stone showed an unusual violet color. The UV-Vis-NIR spectrum (figure 5) showed absorption bands between 500 and 700 nm and a broad band near ~690 nm. This spectrum was consistent with Maxixe beryl (again, see Adamo et al., 2008). While Maxixe beryl has been found to be colored by natural irradiation, it can also be produced by artificial irradiation. Some of these "Maxixe-type" beryls produced by artificial irradiation are known to fade when exposed to "mild heat or strong light" (see Winter 1997 Lab Notes, p. 293). However, there is no conclusive test to determine whether Maxixe color results from natural or artificial irradiation, and as such, beryl in the blue to violet color range that shows the type of visible spectrum previously mentioned is designated simply as the Maxixe variety of beryl by the GIA laboratory.

Figure 4. This 26.72 ct Maxixe beryl has an unusual violet color. Photo by Diego Sanchez.

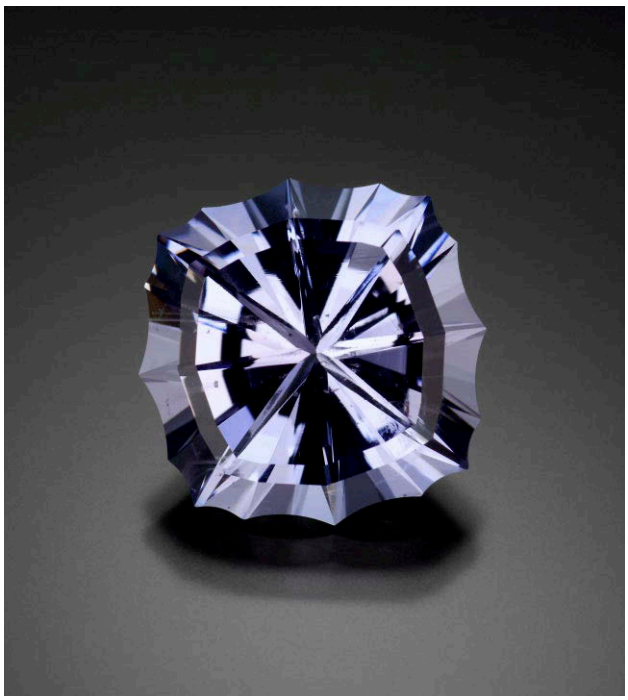

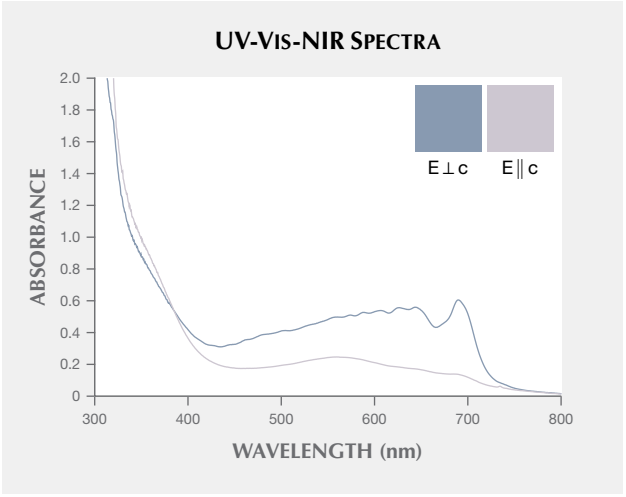

Figure 5. The violet beryl showed a typical UV-Vis-NIR spectrum for Maxixe beryl. Pleochroic colors were calculated from the spectra and revealed a blue (o-ray, dark blue trace and color swatch) and light violet (e-ray, pale purple trace and color swatch) pleochroism.

A small sample cut from the same rough as the 26.72 ct violet beryl was provided by lapidary Nolan Sponsler for destructive testing in order to evaluate the color stability of this material. An optically oriented wafer, 4.45 mm thick and normalized to a 25 mm path length in order to better observe the change in color, was fabricated from this sample with parallel polished windows that are parallel to the optic axis to allow measurement of the o- and e-rays. UV-Vis-NIR spectra were collected on the sample prior to fade testing and at four-hour intervals of exposure to a 150-watt halogen bulb at a distance of approximately four inches from the bulb to avoid any significant heating (figure 6). The results showed fading of the sample until its color was very pale (figure 7), confirming that this material may fade. One should avoid prolonged exposure to light and store it in a dark environment to preserve the color.

This violet Maxixe beryl was purported to be from Santa Maria de Itabira, Minas Gerais, Brazil. It is notable for its unusual color and its fantasy cut design. In addition to this violet Maxixe beryl, another violet beryl group mineral named "johnkoivulaite" was documented in 2019 (see Fall 2019 GNI, pp. 454–455); that new beryl is from the Mogok mining area in Myanmar. However, standard gemo-

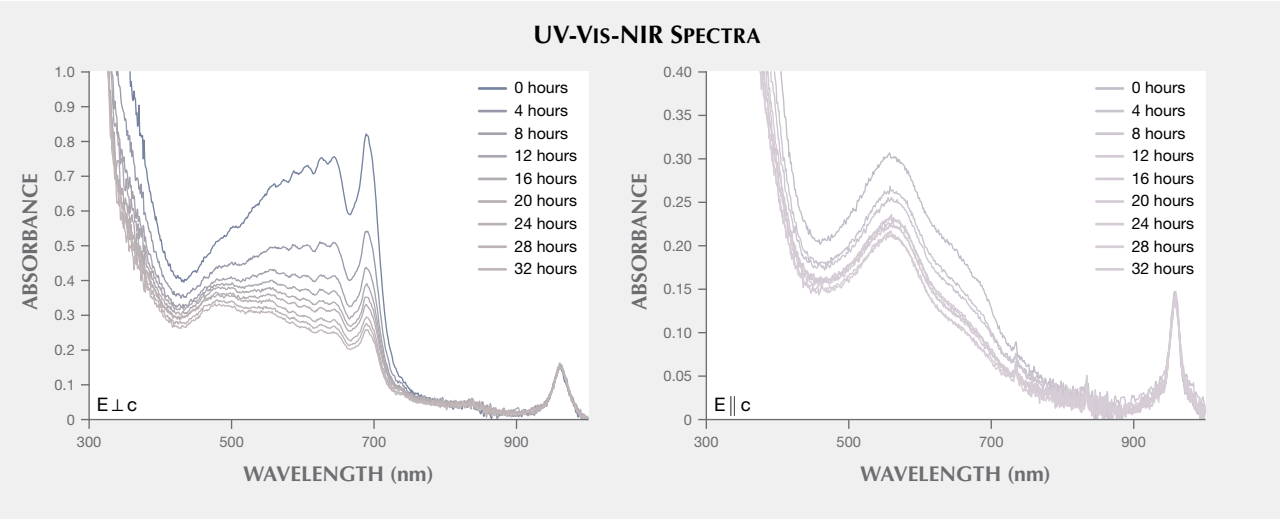

Figure 6. From the violet beryl material provided for this study, a wafer was fabricated in order to directly measure the absorption spectra while conducting a fade test by placing the sample four inches away from an intense 150-watt halogen light source. The results, normalized to a 25 mm path length, confirmed that the color became less saturated over time with exposure to light. Most of the color loss came from the o-ray direction (left).

logical properties clearly separate the two violet beryl minerals. Even though this beryl owes its appealing violet hue to what would be considered an unstable color center, the color should remain intact if prolonged exposure to intense light sources is minimized.

Amy Cooper, Ziyin Sun, Dylan Hand, and Nathan Renfro
GIA, Carlsbad, California

SYNTHETICS AND SIMULANTS

A new type of rutilated quartz composite product. Rutilated quartz, which refers to natural quartz with rutile needle inclusions, is very popular in Taiwan's mineral market. Merchants carve rutilated quartz into spheres rather than pendants or cabochons to get higher prices. The value of such spheres depends on the size of quartz as well as the abundance or appearance of its rutile crystals. Since large and well-formed rutilated quartz is quite rare, it is possible to make those of lower quality into doublets with top covers of glass or synthetic quartz.

Recently, a rutilated quartz sphere was sent to Taiwan Union Lab of Gem Research (TULAB) for certification service. Half of the sphere was colorless and transparent, while the other half was brown and semitranslucent (figure 8). The supplier had informed the client that it was a rutilated quartz polished into a sphere together with its host rock in order to retain the maximum size and the striking rutile inclusions. The colorless and brown parts had refractive

Figure 7. The polarized visible spectra were used to produce color swatches of the ordinary-ray (E ⊥ c) and extraordinary-ray (E || c) color normalized to a 25 mm path length to illustrate the change in color during fade testing over a period of 32 hours at four-hour intervals.

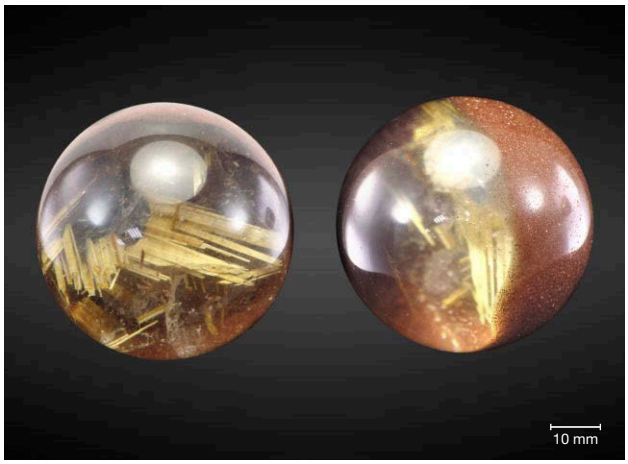

Figure 8. Photos of the rutilated quartz taken in different viewing directions (top view on the left and side view on the right) showed that the sphere was half colorless and half brown. Photos by Shu-Hong Lin.

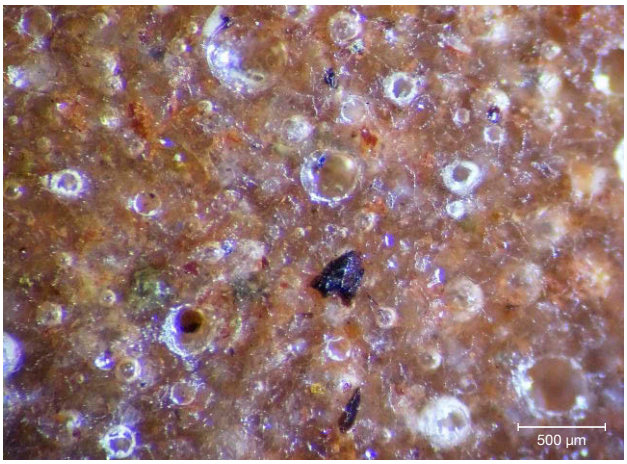

Figure 9. The microscopic image of the brown part of the rutilated quartz sphere showed yellow, brown, and black mineral particles with an abundance of bubbles. Photomicrograph by Shu-Hong Lin.

indices of 1.54 and 1.55, respectively, and the fluorescence was inert under an ultraviolet lamp. Microscopic observation revealed that the brown part contained yellow, brown, and black mineral particles with a large number of bubbles (figure 9). The specific gravity was 2.35, which is much lower than the specific gravity of quartz. To further confirm the material of the sphere, the colorless and brown parts were analyzed with a Raman spectrometer. The results showed that the former was quartz, and the latter was mainly composed of epoxy resin and quartz (figure 10).

After a series of gemological tests, we concluded that this sphere could be defined as a new type of doublet or composite material of rutilated quartz, in which the brown part mistaken for host rock was in fact epoxy resin mixed

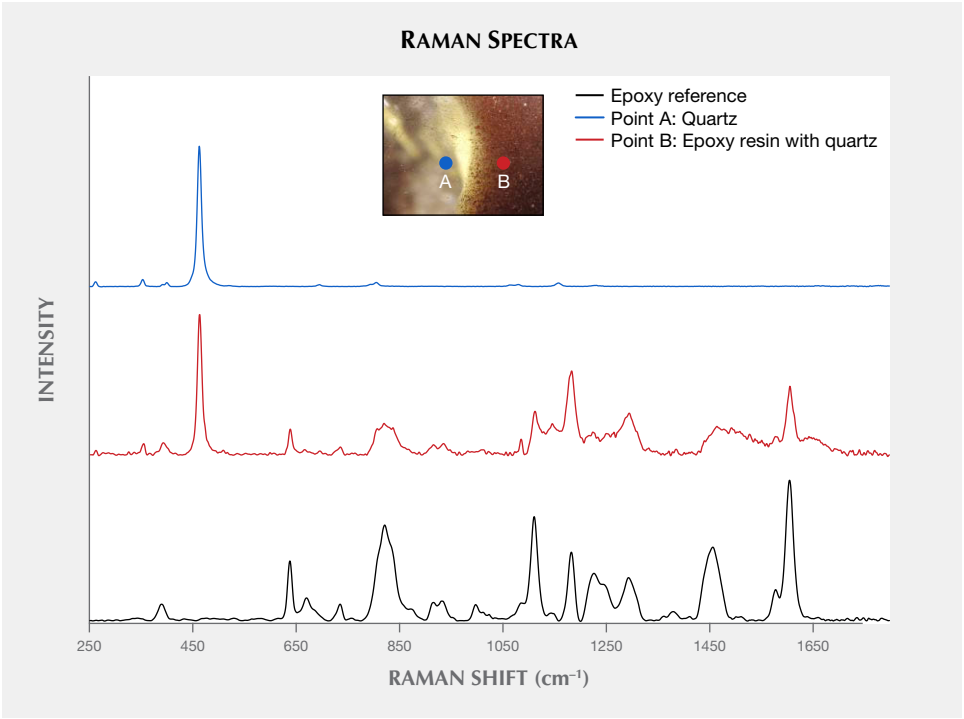

Figure 10. Stacked Raman spectra of the rutilated quartz sphere and epoxy resin revealed that the colorless part (A) was quartz (463 cm^{-1}) and the brown part (B) was mainly composed of epoxy resin (peaks at 637, 822, 1113, 1182, and 1606 cm^{-1}) and quartz. The spectra are baseline-corrected and normalized.

with mineral powders. Due to the increasing demand for rutilated quartz spheres in Taiwan, this composite material may not be merely an isolated case.

Shu-Hong Lin
Institute of Earth Sciences,
National Taiwan Ocean University
Taiwan Union Lab of Gem Research, Taipei
Yu-Ho Li
Institute of Earth Sciences,
National Taiwan Ocean University
Huei-Fen Chen
Institute of Earth Sciences and
Center of Excellence for Oceans
National Taiwan Ocean University, Keelung, Taiwan

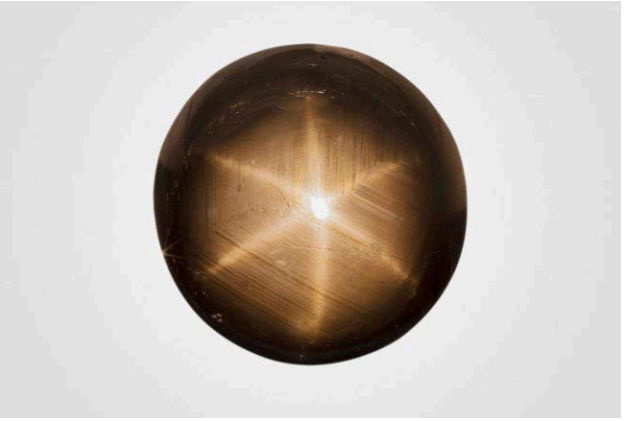

Figure 11. The 75 ct black star sapphire that was brought in for testing. Photo by Wimon Manorotkul.

TREATMENTS

Black star sapphire with dual treatments. Black star sapphires primarily come from Kenya, Australia, and Thailand. Unlike other star sapphires and rubies, the asterism in these stones generally results from the exsolution of ilmenite ($FeTiO_3$) and/or hematite (α-Fe_2O_3) instead of rutile (TiO_2). Rutile and ilmenite/hematite exsolve in different directions: rutile along the second-order hexagonal prism $\{11\bar{2}0\}$ and ilmenite along the first-order hexagonal prism $\{10\bar{1}0\}$. If both are present in the same stone, a 12-ray star results. The ilmenite/hematite crystals are far more "platy," and thus their layers tend to form planes of weakness. Breakage along those planes is termed parting. Parting differs from cleavage in that it results from structural planes of weakness due to imperfect growth rather than inherent weakness. There are often two different parting planes in the stones. One corresponds to the exsolution of ilmenite/hematite in the plane of the basal pinacoid {0001}. The other corresponds to planes of exsolved boehmite/diaspore along the rhombohedron $\{10\bar{1}1\}$.

In Thailand, one often sees cavities on the back of black star sapphires filled in with brown dopping varnish. It is only the basal parting that comes into play with black star sapphires, because the exsolved hematite that causes the lack of adhesion is only in the basal plane. It is because of this parting that the stones get filled with dopping varnish, to conceal large holes in the base. Note that the type of dopping varnish is of a color that matches the stone.

In May 2020, a client submitted a large 75 ct black star sapphire for testing (figure 11). The base of the stone contained two large pits filled with brown dopping shellac (figure 12, left). Interestingly enough, the shellac fluoresced bright orange under long-wave ultraviolet light (365 nm) (figure 12, right). Following the client's approval, we removed the shellac with alcohol and noticed a curved area exhibiting an unusual flow-like structure that looked suspiciously like glass. Unfortunately, attempting to get a Raman spectrum on the area was unsuccessful.

Careful microscopic examination showed what looked like gas bubbles trapped between the glassy material and the sapphire below (figure 13). Scratching the surface of the cavity with a number 7 hardness point confirmed that the area could not be corundum. Immersing the gem in methylene iodide showed the glassy area to cover roughly two-thirds of the base of the cabochon (figure 14). Energy-dispersive x-ray fluorescence (EDXRF) testing on the area suspected to be glass revealed a lead (Pb) component of over 3%.

Figure 12. Left: Two large pits on the base of the star sapphire contain brown dopping varnish (the white areas are adhesive from tape). Field of view 30 mm. Right: Under long-wave ultraviolet light (365 nm), the dopping shellac fluoresced bright orange. Field of view 27 mm. Photomicrographs by Richard W. Hughes.

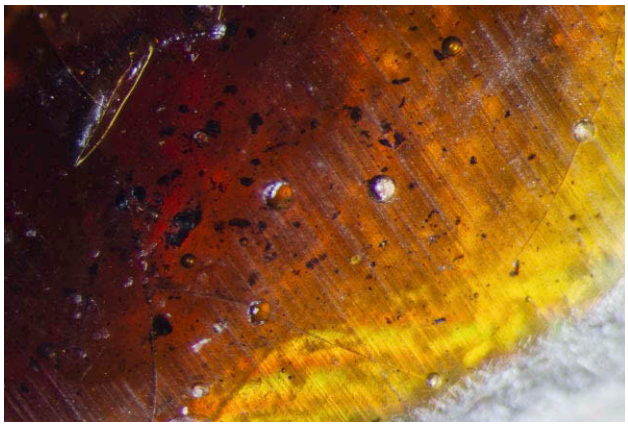

Figure 13. A close-up view of the shellac in the lower pit revealed trapped gas bubbles and black debris. Photomicrograph by Richard W. Hughes; field of view 5 mm.

Figure 14. Immersion in methylene diiodomethane (n = 1.741) reveals the extent of the glass filling on the base of the cabochon (the dark area that spreads across a large portion of the base). Photomicrograph by Richard W. Hughes; field of view 30 mm.

A variety of tests were brought to bear on this specimen, from the simple (hardness) to the high-tech (EDXRF). The results of these tests revealed a gem that had been treated by filling with two different substances: glass and dopping varnish.

Richard W. Hughes, E. Billie Hughes, and Wimon Manorotkul
Lotus Gemology, Bangkok

Oiled spinel. When it comes to clarity enhancement with oils and resins, a common belief is that the refractive index of the host gem must match that of the filler. If one follows this logic, it would seem that using oils or resins to clarity enhance corundum (n = 1.76) or spinel (n = 1.72) would not be at all effective, since there is a yawning gap in RI between those gems and that of any oil or resin.

Certainly, Burmese gem traders have never bought into that idea, for we regularly encounter oiled rubies, sapphires, and spinels from Myanmar. In fact, Burmese traders have told us that it is common practice to immediately immerse rough into oil after it is unearthed (figure 15). Oiling rough not only makes viewing the interior easier but also significantly enhances the gem's clarity. In our experience, such treatment is almost never disclosed to buyers.

Figure 15. Bojan brand "King Ruby Red Oil" from Chanthaburi, Thailand, along with a parcel of rough Thai rubies purchased by the author in 2016. Note the red stain on the plastic bag. Photo by Wimon Manorotkul.

In 2013, while visiting various mines and markets in Myanmar's Mogok Stone Tract, we were taken to a small house where a man was heat-treating spinel. Gems were placed in a crucible and heated for a period of time. Then, while still relatively hot, they were dumped into a vessel containing red oil. It was a remarkable piece of performance art. After the oil was wiped off, we could discern no change in color from the heating.

Because of the prevalence of oiling, we now check every stone with fissures for oil, no matter the origin or type of gem. This is typically done with a hot point under the microscope. The hot point gently heats the gem until, with oiled stones, the oil leaks out of the fissure in beads on the surface of the stone. With the exception of emerald, customers purchasing colored gems are not expecting them to be clarity enhanced. As one major Bangkok trader told us several years ago, "I cannot sell an oiled spinel." For this reason, when we determine that a gem other than emerald has been fissure-filled with an oil or resin, we notify the client and allow them two opportunities to remove the filler before we issue the report.

In September 2020, Lotus Gemology received for identification a 3 ct spinel that originated from Mogok. We noticed a fissure on the pavilion running parallel to the girdle plane, and application of the hot point caused oil to leak out. After two rounds of oil removal by the client, the difference was truly remarkable. The gem was now disfigured by a highly reflective eye-visible fissure (figure 16).

This clearly demonstrates that oil can have a significant impact on the clarity of a gem even when there is a big difference in RI between the host and the oil. The greatest impact will be found in stones like this spinel, where fissures lie perpendicular to the viewing angle.

Richard W. Hughes
Lotus Gemology, Bangkok

CONFERENCE REPORTS

GSA Annual Meeting: Gem Research Session. The Geological Society of America held its 2020 annual meeting as a virtual conference October 26–30 (figure 17). The session on gemological research took place on Thursday, October 29, and featured presentations on various gemological topics.

Nelson Eby from the Department of Environmental, Earth, and Atmospheric Sciences of the University of Massachusetts in Lowell presented a chemical classification of emeralds from 24 deposits in 10 countries. Using data on major and minor chemical elements in emeralds obtained by the instrumental neutron activation analysis, he demonstrated how these emerald occurrences could be grouped into deposits related to igneous processes, to those related to low-to-moderate temperature solutions in sedimentary environments, and to metamorphic processes. **Rhiana Henry** of the Department of Earth, Ocean, and Atmospheric Sciences of the University of British Columbia in Vancouver described a method that could be used to calculate the water content of an emerald based on measured values of either Na^+ atoms per formula unit (apfu) or weight percent Na_2O. **Cisil Badur** of the Department of Geosciences at Auburn University in Alabama investigated plagioclase megacrysts containing macroscopic inclusions of native copper from the Dust Devil mine in south-central Oregon. She concluded that the homogeneous distribution of major and trace elements (including Cu) in the feldspar resulted from a rapid rate of cooling of the host basalt (which prevented substantial internal chemical diffusion following initial crystallization). The megacrysts display anomalously young argon-argon (or $^{40}Ar/^{39}Ar$) ages, which she attributed to the loss of radiogenic argon. **Shiyun Jin** of GIA in Carlsbad, California, investigated the thin, oriented, ribbon-like inclusions of magnetite and hematite whose presence cre-

Figure 16. On the left is the 3 ct spinel as initially submitted. At right is the same stone after removal of the oil. The difference is striking. Following cleaning, a large reflective fissure is visible parallel to the girdle plane. This demonstrates the ability of an oil/resin to mask fissures even when there is no close match in refractive index between the filler and host. Photos by Chanon Yimkeativong/Lotus Gemology.

Figure 17. The 2020 annual meeting of the Geological Society of America was held online this year due to the Covid-19 pandemic. Courtesy of GSA and Image AV/e-Attend.

ates an aventurescence effect in some rainbow lattice sunstone from Australia. The iron in these inclusions is thought to have been initially dissolved in the feldspar lattice and then expelled during exsolution of albite (as lamellae) and ordering of the crystal structure during cooling of the host orthoclase.

A study of zircon inclusions in unheated sapphires from four important commercial metamorphic deposits was carried out by **Wenxing Xu** from the Gübelin Gem Lab in Lucerne, Switzerland. She demonstrated how Raman spectroscopic features can help distinguish geologically younger sapphires from Kashmir and Myanmar from geologically older samples from Sri Lanka and Madagascar. **Wim Vertriest** of GIA in Bangkok discussed the identification of opaque sulfide inclusions in rubies. Inclusions in marble-hosted rubies from Mogok, Myanmar, proved to be pyrrhotite and sphalerite, while those from amphibole rocks in Montepuez, Mozambique, were complex mixtures of Fe-Cu-Ni sulfide minerals, which suggests differences in the geological conditions of ruby formation. **Evan Smith** from GIA in New York discussed the genetic relationship between type IIb and certain type IIa diamonds. Both types appear to have formed in the sublithospheric mantle with the involvement of subducted serpentinized peridotite.

Ping Ma of the China University of Geosciences in Wuhan discussed the value of using three-dimensional fluorescence spectra to help differentiate untreated and various treated jadeite samples in the marketplace. **Di Cui** of the Engineering Research Center of Gems and Technological Materials of Tongji University in Shanghai described the chemical composition and crystal structure of both the emeralds from the Davdar deposit in Xinjiang Province of northwest China, and in a separate presentation, the high vanadium-content emeralds from the Dayakou deposit of Malipo County in southwestern China. **Elina Myagkaya** of GIA in New York described an unusual brownish yellow diamond that was found to be a IIa + IIb mixed-type diamond. Investigation using cathodoluminescence and photoluminescence hyperspectral imaging revealed a complex growth pattern distinguished by differences in luminescence colors and various optical defects.

James E. Shigley
GIA, Carlsbad, California